PNAS RESEARCH ARTICLE | NEUROSCIENCE

The spectral sensitivity of human circadian phase resetting and melatonin suppression to light changes dynamically with light duration

Melissa A. St Hilaire[a,b,1], María L. Ámundadóttir[c,1], Shadab A. Rahman[a,b], Shantha M. W. Rajaratnam[a,b,d], Melanie Rüger[a,b], George C. Brainard[e], Charles A. Czeisler[a,b], Marilyne Andersen[c], Joshua J. Gooley[a,b,f], and Steven W. Lockley[a,b,2]

Edited by Joseph Takahashi, The University of Texas Southwestern Medical Center, Dallas, TX; received March 25, 2022; accepted November 3, 2022

Human circadian, neuroendocrine, and neurobehavioral responses to light are mediated primarily by melanopsin-containing intrinsically-photosensitive retinal ganglion cells (ipRGCs) but they also receive input from visual photoreceptors. Relative photoreceptor contributions are irradiance- and duration-dependent but results for long-duration light exposures are limited. We constructed irradiance-response curves and action spectra for melatonin suppression and circadian resetting responses in participants exposed to 6.5-h monochromatic 420, 460, 480, 507, 555, or 620 nm light exposures initiated near the onset of nocturnal melatonin secretion. Melatonin suppression and phase resetting action spectra were best fit by a single-opsin template with lambda$_{max}$ at 481 and 483 nm, respectively. Linear combinations of melanopsin (ipRGC), short-wavelength (S) cone, and combined long- and medium-wavelength (L+M) cone functions were also fit and compared. For melatonin suppression, lambda$_{max}$ was 441 nm in the first quarter of the 6.5-h exposure with a second peak at 550 nm, suggesting strong initial S and L+M cone contribution. This contribution decayed over time; lambda$_{max}$ was 485 nm in the final quarter of light exposure, consistent with a predominant melanopsin contribution. Similarly, for circadian resetting, lambda$_{max}$ ranged from 445 nm (all three functions) to 487 nm (L+M-cone and melanopsin functions only), suggesting significant S-cone contribution, consistent with recent model findings that the first few minutes of a light exposure drive the majority of the phase resetting response. These findings suggest a possible initial strong cone contribution in driving melatonin suppression and phase resetting, followed by a dominant melanopsin contribution over longer duration light exposures.

circadian rhythms | circadian phase resetting | melatonin suppression | light | melanopsin

Significance

Using data from 100 healthy young participants studied during a 9-d inpatient protocol, we constructed analytic action spectra for melatonin suppression and circadian phase resetting in response to 6.5-h monochromatic light exposures and fit these action spectra with linear combinations of melanopsin (ipRGC), short-wavelength (S), and combined long and medium-wavelength (L+M) cone functions. First, we demonstrate that melatonin suppression is driven approximately equally by S and L+M cones in the first quarter of light exposure and melanopsin only over longer durations. Second, we demonstrate that S cones may contribute significantly to the overall phase resetting given the nonlinear relationship between light duration and magnitude of resetting. These findings indicate that the spectral sensitivity of circadian light responses changes over time.

The circadian system ensures that daily rhythms of human behavior and physiology are aligned appropriately with the solar day. Photic entrainment of circadian rhythms is mediated by direct retinal projections to the circadian pacemaker in the suprachiasmatic nucleus (SCN) of the hypothalamus (1). The SCN, in turn, regulates multiple other circadian-controlled functions, including circadian synthesis of melatonin in the pineal gland (2). In addition to resetting the circadian phase of the melatonin rhythm, exposure to light during the biological night acutely inhibits melatonin synthesis (3, 4). Light therefore plays a critical role in regulating melatonin levels, with potential effects on sleep behavior, immune function, glucose metabolism, and other systems (5–8).

Over the past twenty years, there has been substantial progress in characterizing the photoreceptor pathways that regulate circadian rhythm resetting and melatonin suppression. Intrinsically photosensitive retinal ganglion cells (ipRGCs) contain the photopigment melanopsin, which is most sensitive to short-wavelength light in the blue portion of the visual spectrum (lambda$_{max}$ = 480 nm) (9–13). The ipRGCs also receive input from rod and cone photoreceptors in the outer retina (14–16), however, suggesting that both melanopsin and visual photoreceptors contribute to non-image-forming light responses. This multi-photoreceptor involvement in circadian responses is supported by findings in mice: circadian phase shift responses are preserved in both visually blind mice with intact ipRGCs and melanopsin-deficient mice with intact vision (10, 11, 17, 18). Circadian responses to light are eliminated only when all photoreceptor types are rendered dysfunctional (10). Similarly, human phase resetting and melatonin suppression responses are short-wavelength sensitive (19, 20) and persist in the absence of functional rods and cones (21–23), but also respond to long-wavelength light in sighted individuals beyond the expected sensitivity of melanopsin activation alone (24). Converging lines of evidence in rodents and data for a limited number of wavelength responses in humans suggest that visual photoreceptors contribute substantially to circadian responses at lower irradiances and during the early

Author contributions: S.A.R., M.R., G.C.B., C.A.C., J.J.G., and S.W.L. designed research; S.A.R., S.M.W.R., M.R., J.J.G., and S.W.L. performed research; M.A.S., M.L.A., S.A.R., M.A., J.J.G., and S.W.L. analyzed data; and M.A.S., M.L.A., S.A.R., S.M.W.R., M.R., G.C.B., C.A.C., M.A., J.J.G., and S.W.L. wrote the paper.

The authors declare no competing interest directly related to the work presented in this manuscript. A full list of potential competing interests has been provided in the SI Appendix.

This article is a PNAS Direct Submission.

[1]M.A.S. and M.L.A. contributed equally to this work.

[2]To whom correspondence may be addressed. Email: slockley@hms.harvard.edu.

This article contains supporting information online at https://www.pnas.org/lookup/suppl/doi:10.1073/pnas.2205301119/-/DCSupplemental.

Published December 12, 2022.

part of a light exposure, whereas melanopsin is the primary circadian photopigment at higher irradiances and for longer-duration light exposures (24–26).

Although our prior work suggests complementary roles for melanopsin and rod-cone photoreceptors in mediating non-visual light responses (24), there has yet to be a comprehensive evaluation of the spectral sensitivity for these responses over longer durations than the initial seminal 30- and 90-min exposure action spectra for melatonin suppression in humans (19, 20). Under typical conditions, humans are exposed to extended photoperiods during the 'day' (natural plus man-made) and often at night, for example during shiftwork, which requires light exposures over many hours. To address these gaps in our knowledge, we used analytic action spectroscopic techniques to identify and model the contributions of different human photopigments to circadian phase resetting and light-induced suppression of melatonin overnight. We show that phase resetting and melatonin suppression responses are broadly short-wavelength sensitive for long-duration (6.5 h) exposure to light but that, at the start of a light exposure, melatonin suppression is best explained by combined contributions of melanopsin and visual photoreceptors.

Results

Dynamics of Spectral Sensitivity for Melatonin Suppression in Constant Light. We measured melatonin suppression in 99 young healthy participants (34 female, 65 male, 22.9 ± 2.9 y) exposed to 6.5 h of continuous monochromatic light during the biological night (420 nm, n= 9; 460 nm, n = 30; 480 nm, n = 11; 507 nm, n = 8; 555 nm, n = 33; 620 nm, n = 4; dark controls, n = 4). Within each wavelength group, participants were randomized to receive a fixed-irradiance light exposure (half-peak bandwidth = 10–14 nm) following mydriasis starting near the onset of melatonin secretion using a modified Ganzfeld dome (19, 24), with photon densities ranging from 2.52×10^{11} to 1.53×10^{14} photons/cm^2/sec. Data for 460 nm, 555 nm, controls, and two of the 11 participants for 480 nm have been published previously (24).

Melatonin suppression for the entire 6.5 h was calculated from the reduction in melatonin area under the curve during the light exposure as a percentage of the corresponding value in dim light 24 h earlier. Overall, the amount of melatonin suppression increased with increasing irradiance at each wavelength (Fig. 1 *A*–*F*). Irradiance response curves for each wavelength were fit with a four-parameter logistic function with fixed values for the upper and lower asymptotes (95 and 0%, respectively) but variable slope (i.e., non-univariant; R^2 range 0.60–0.93; Fig. 1 *A*–*F*). The darkness control data were included in every fit. The model fit did not converge for the 620 nm data. The ED_{50} values for each wavelength were then converted to a relative sensitivity and fitted with a Govardovskii opsin template to determine the peak sensitivity. The resultant action spectra using the ED_{50} values from the non-univariant fits (Fig. 1*G*) had a single-opsin best-fit $lambda_{max}$ of 482 nm (mean absolute error, MAE = 0.21), which shifted to 481 nm (MAE = 0.13) after adjusting for the lens transmission of a 22-y-old observer (27, 28) (*SI Appendix*, Fig. S1*A*).

To model photoreceptor contributions to overall melatonin suppression, the resultant action spectrum was also fitted with a combination of ipRGC, S cone, and L+M cone opsin curves. We did not fit combinations that included a rhodopsin curve because our dataset is underpowered to differentiate between opsins with peaks at 480 nm and 507 nm. The ipRGC and S cone sensitivity curves were obtained using the Govardovskii opsin template with a $lambda_{max}$ of 480 nm and 419 nm, respectively (*SI Appendix*, Fig. S1*B*), which shift to 484 nm and 439 nm, respectively, when corrected for the lens transmittance of a 22-y-old observer (*SI Appendix*, Fig. S1*C*). Given the sparse data distribution (five ED_{50} values) and that the sensitivity of the L- and M-cones overlap significantly ($lambda_{max}$ of 558 nm and 531 nm), their response

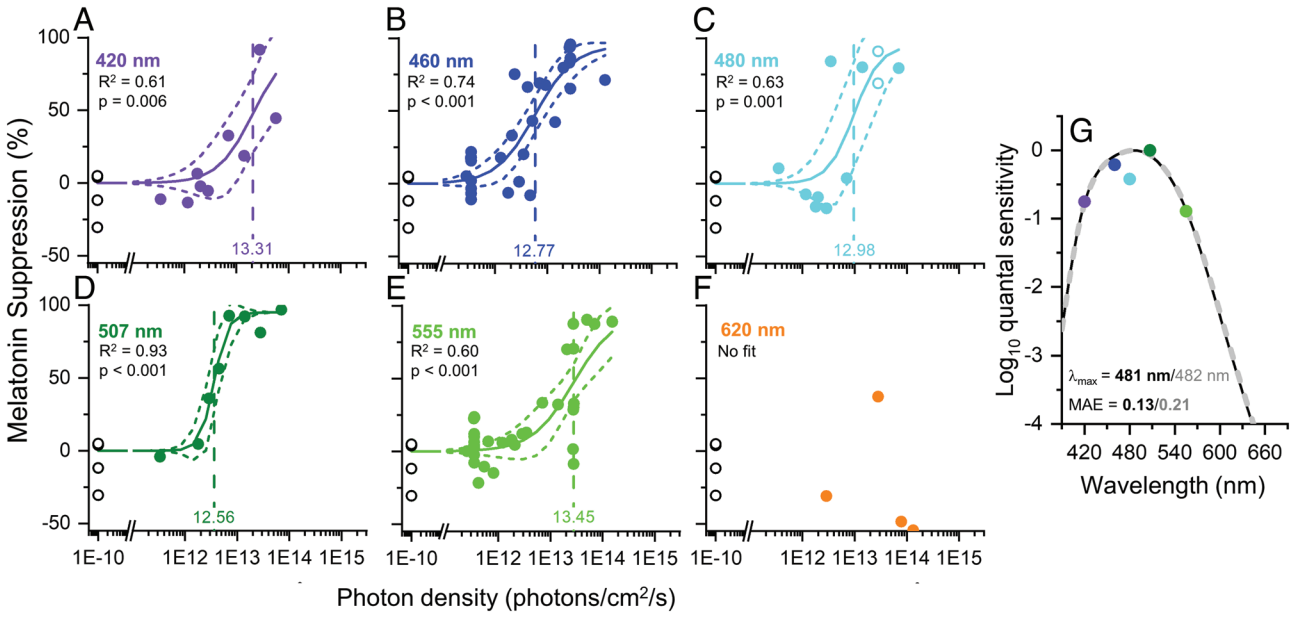

Fig. 1. Best-fit dose response curves for melatonin suppression across 6.5 h of light exposure. (*A*–*F*) The best-fit dose response curves for melatonin suppression in response to 6.5 h of light exposure as a function of photon density for monochromatic wavelengths of 420 (n = 9), 460 (n = 30), 480 (n = 11), 507 (n = 8), 555 (n = 33), and 620 nm (n = 4). The minimal and maximal responses were fixed at 0% and 95%, respectively; the ED_{50} and slope were allowed to vary. The $log_{10}ED_{50}$ values (vertical dashed line) ranged from 12.56 to 13.45 photons/cm^2/sec and the slopes ranged from 1.10 to 3.29. The adjusted R^2 values for the fits ranged from 0.60 to 0.93. The n = 4 darkness controls plotted at $1e^{-10}$ photons/cm^2/sec were included in the fits for all wavelengths. The data for 620 nm (panel *F*) were not fit due to the small sample size in this group. (*G*) Action spectra for long-duration melatonin suppression responses. The full dataset best matches a Govardovskii opsin template with $lambda_{max}$ = 481 nm (MAE = 0.13; solid black line), assuming a correction for lens transmission of a 22-y-old individual; the best-fit opsin without lens transmission correction is shown in the dashed gray line for comparison ($lambda_{max}$ = 482 nm; MAE = 0.21).

was modeled as a weighted sum (2:1 ratio) (29) with maximum absorbance at 548 nm. Fig. 2 shows the MAE and rootmean square error (RMSE)-derived best fit of the pairwise linear combinations of ipRGCs, S cones, and L+M cones (2-channel; Fig. 2 *D–F*) and the linear combination of all three (ipRGCs, S cones and L+M cones, 3-channel; Fig. 2*G*) compared to ipRGCs alone (1-channel; Fig. 2 *A–C*) on overall melatonin suppression in response to a 6.5-h light exposure. Based on MAE and RMSE, the three-channel model provided the best fit to the data (MAE = 0.11; RMSE = 0.16), with the majority of the contribution from ipRGCs (81%), followed by S cones (12%) and L+M cones (7%).

Similar analyses were conducted using the ED_{90} value of the non-univariant fits from Fig. 1. The ED_{90} value more closely reflects the maximal response of the system at each wavelength. Based on MAE and RMSE, the ED_{90} response for melatonin suppression is dominated by the ipRGCs with no contributions from S cones or L+M cones (MAE = 0.22, RMSE = 0.28; *SI Appendix*, Fig. S2). It should be noted, however, that the ED_{90} value extended beyond our experimental data for 420 nm and 555 nm and was extrapolated based on the model fits, which limits our ability to interpret these data.

To estimate the change in photoreceptor contribution to melatonin suppression over time (24), we constructed irradiance response curves for each quarter of the exposure (97.5-min intervals) and applied the same four-parameter logistic function with fixed upper and lower asymptotes and variable slope to each wavelength over each quarter (*SI Appendix*, Fig. S3). The resultant action spectra using the ED_{50} values for each quarter were fitted with a combination of ipRGC, S cone, and L+M cone opsin curves as described above. Fig. 3 shows the linear combination of ipRGCs and S cones (2-channel; Fig. 3 *E–H*), ipRGCs and L+M cones (2-channel; Fig. 3 *I–L*), and ipRGCs, S cones, and L+M cones (3-channel; Fig. 3 *M–P*) compared to ipRGCs alone (1-channel; Fig. 3 *A–D*) across all four quarters; other single-opsin and pairwise linear combinations are reported in *SI Appendix*, Fig. S4. For the combined ipRGC and S cone fits (Fig. 3 *E–H*), the peak sensitivity for the first quarter of the light exposure was 476 nm, which is slightly shorter than the peak of melanopsin alone (484 nm), and with a 21% contribution from the S cones. From the second quarter and for the remainder of the light exposure, the peak sensitivity moved closer to that of melanopsin (478 to 484 nm), with a contribution of 82 to 100% from the ipRGCs, suggesting a stable, dominant contribution of melanopsin alone in mediating the sustained suppression response, and consistent with the overall 6.5-h light exposure response (Fig. 2). For the combined ipRGC, S, and L+M cone fits (Fig. 3 *M–P*), however, a more complex pattern emerged. For the first quarter of the light exposure, the suppression was consistent with substantial contributions from S and L+M cones (51% and 47% contributions, respectively), resulting in a fit with an overall peak sensitivity of 441 nm, and a secondary peak sensitivity of 550 nm. Over time, however, the relative contribution of the ipRGCs increased and that of the S and L+M cones decreased such that for the second half of the light exposure, the response was dominated by the ipRGCs (79 to 92%) with a final peak sensitivity of 485 nm in the fourth quarter, which is consistent with a melanopsin response alone and minimal

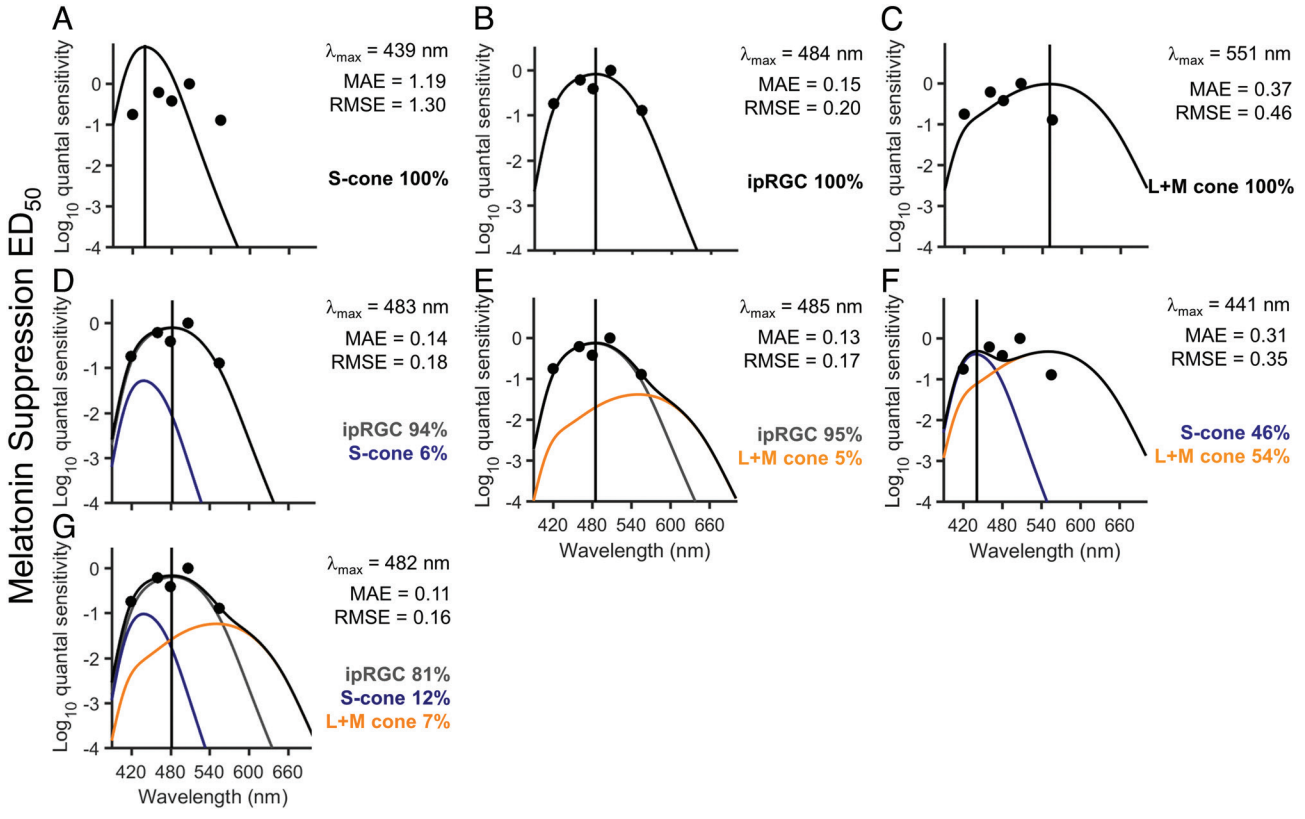

Fig. 2. Linear combinations of opsin fits to melatonin suppression across 6.5 h of light exposure. (*A–C*) The S-cone (*A*), ipRGC (*B*), and L+M opsin template (*C*) reflecting correction for lens transmission plotted against the relative quantum sensitivities derived from the $log_{10}ED_{50}$ values for the overall 6.5-h light exposure for melatonin suppression. (*D–G*) The best-fit linear combinations of ipRGCs and S cones (*D*), ipRGCs and L+M cones (*E*), S cones and L+M cones (*F*), and ipRGCs, S cones, and L+M cones (*G*). In each panel, the gray solid line represents the ipRGC sensitivity curve, the blue solid line represents the S cone sensitivity curve, and the orange solid line represents the L+M cone sensitivity curve, whereas the black solid line shows the sum of the sensitivity curves, i.e., the best fit through the data points. The $lambda_{max}$ (vertical solid line) reported in each panel indicates the peak sensitivity of the best-fit sensitivity curve. The percentages represent the relative contribution of each spectral sensitivity curve to the overall sensitivity. The MAE and RMSE of the best fits are reported for each model.

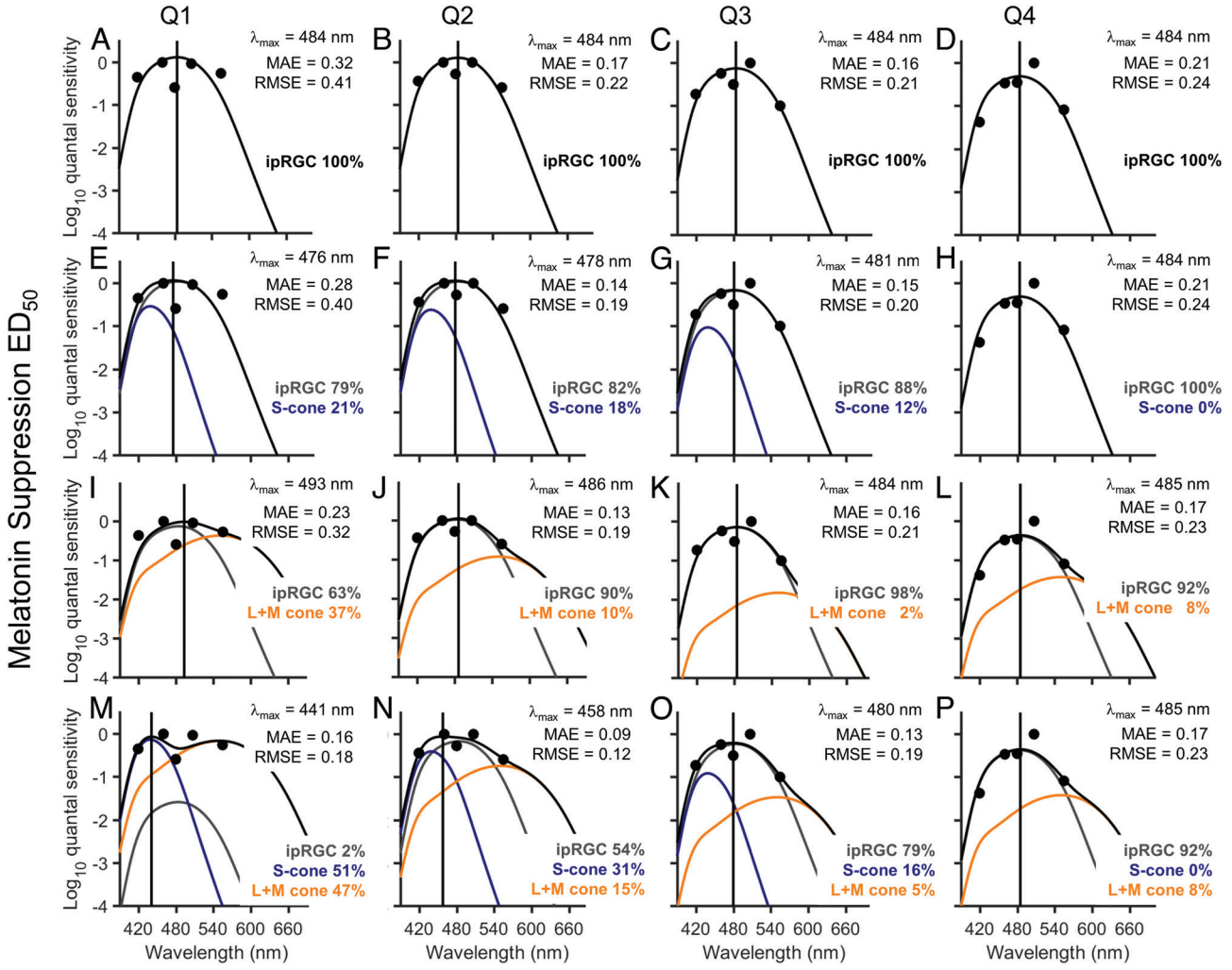

Fig. 3. Linear combinations of opsin fits to melatonin suppression across each quarter of light exposure. (*A–D*) The ipRGC opsin template (lambda$_{max}$ = 480 nm; shifted to 484 nm after correction for lens transmission of a 22-y-old individual) plotted against the relative quantum sensitivities derived from the $\log_{10}ED_{50}$ values for each quarter (Q1-4) of a 6.5-h light exposure for melatonin suppression. (*E–H*) The best-fit linear combination of ipRGCs and S cones, (*I–L*) ipRGCs and L+M cones, and (*M–P*) ipRGCs, S cones, and L+M cones. In each panel, the gray solid line represents the ipRGC sensitivity curve, the blue solid line represents the S cone sensitivity curve, and the orange solid line represents the L+M cone sensitivity curve, whereas the black solid line shows the sum of the sensitivity curves, i.e., the best fit through the data points. The lambda$_{max}$ reported in each panel indicates the peak sensitivity of the best-fit sensitivity curve. The MAE and RMSE of the best fits are reported for each model.

contribution from the cones (Fig. 3*P*). Based on MAE and RMSE, the three-channel model provided the best fit to the data over each quarter (MAE = 0.09 to 0.17; RMSE = 0.12 to 0.23). The time course of the contributions from the combined ipRGC, S, and L+M cone fits is plotted in *SI Appendix*, Fig. S5.

Short-wavelength Sensitivity for Photic Circadian Phase Resetting. We also calculated the circadian phase resetting response in 100 young healthy participants (35 female, 65 male, 22.8 ± 2.9 y) for each exposure (420 nm, n = 10; 460 nm, n = 31; 480 nm, n = 12; 507 nm, n = 8; 555 nm, n = 31 620 nm, n = 4; dark controls, n = 4) as the difference in clock time in the timing of DLMO in the melatonin cycle immediately before and after the light exposure night, as measured during constant routine procedures (24). Irradiance responses curves for each wavelength were fit with a four-parameter logistic function as described for melatonin suppression with fixed values for the upper and lower asymptotes (0.05 and −3.3 h, respectively) but variable slope (R^2 range 0.46 to 0.79; Fig. 4 *A–F*). The darkness control data were included in every fit. The magnitude of the circadian phase delay shift increased with increasing irradiance at each wavelength (Fig. 4 *A–F*). Subsequent analyses were conducted both with and without the 620 nm data (Fig. 4*F*) given the small number of points included in the 620 nm curves. The resultant action spectrum using the ED_{50} values from the non-univariant fits without the 620 nm data included (Fig. 4*G*) had a single-opsin best-fit lambda$_{max}$ of 485 nm (MAE = 0.24), which shifted to 483 nm (MAE = 0.26) after adjusting for the lens transmission of a 22-y-old observer (*SI Appendix*, Fig. S1*A*). When the 620 nm data were included (Fig. 4*H*), the lambda$_{max}$ was 522 nm, which shifted to 521 nm after adjusting for the lens transmission of a 22-y-old observer, but the overall fit was weaker (MAE = 0.39 and MAE = 0.41, without and with correction for lens transmission, respectively).

The same 1-channel, 2-channel, and 3-channel photoreceptor combinations as described above for melatonin suppression were applied to the phase resetting data both with (Fig. 5 *A–G*) and without (*SI Appendix*, Fig. S6 *A–G*) the 620 nm data. While the peak sensitivity (lambda$_{max}$) and proportional photoreceptor contributions did not change substantially when the 620 nm data were included or excluded, the model fits were substantially improved without the 620 nm data (*SI Appendix*, Fig. S6), and

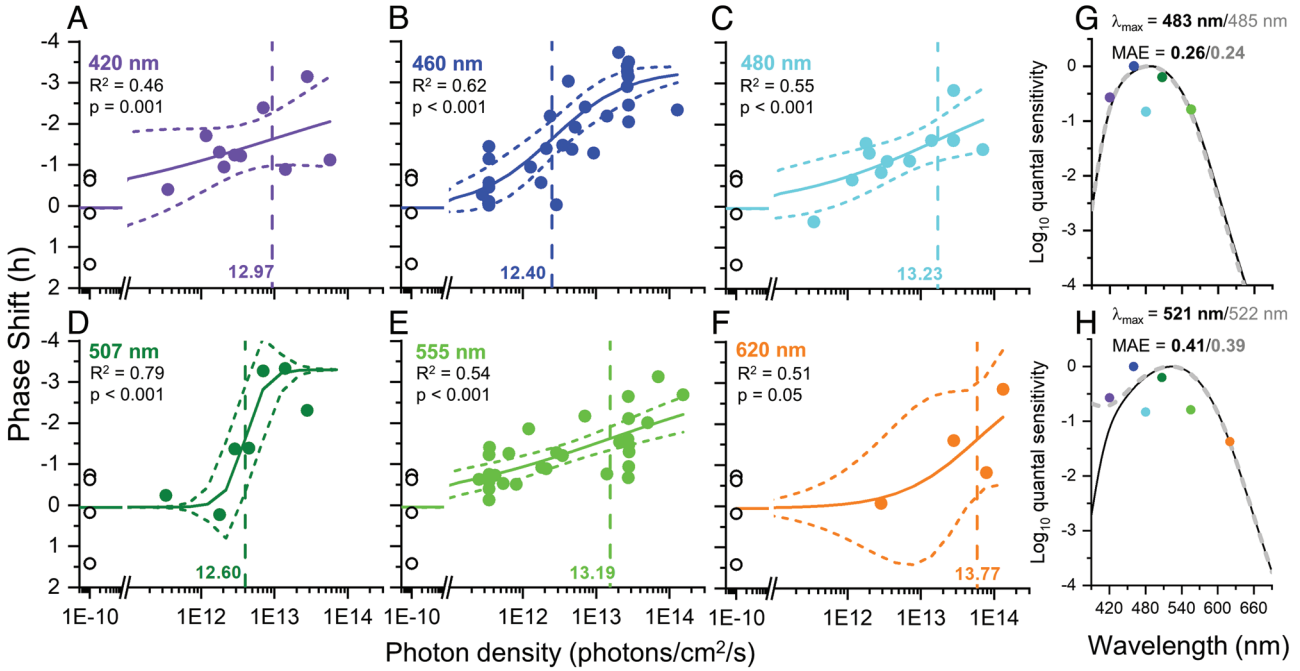

Fig. 4. Best-fit dose response curves for phase resetting across 6.5 h of light exposure. (*A*–*F*) The best-fit dose response curves for phase resetting in response to 6.5 h of light exposure as a function of photon density for monochromatic wavelengths of 420 (n = 10), 460 (n = 31), 480 (n = 12), 507 (n = 8), 555 (n = 31), and 620 nm (n = 4). Phase delays are represented as negative values. The minimal and maximal responses were fixed at 0.05 and −3.3 h, respectively; the ED_{50} and slope were allowed to vary. The $\log_{10}ED_{50}$ values ranged from 12.40 to 13.77 photons/cm^2/sec (vertical dashed line) and the slopes ranged from 0.80 to 3.29. The adjusted R^2 values for the fits ranged from 0.46 to 0.79. The n = 4 darkness controls plotted at $1e^{-10}$ photons/cm^2/sec were included in the fits for all wavelengths. (*G* and *H*) Action spectra for the phase resetting responses. When the 620 nm data are not included, the full dataset best matches a Govardovskii opsin template with $lambda_{max}$ = 483 nm (MAE = 0.26; solid black line), assuming a correction for lens transmission of a 22-y-old individual (Panel *G*); the best-fit opsin without lens transmission correction is shown in the dashed gray line for comparison ($lambda_{max}$ = 485 nm; MAE = 0.24). When the 620 nm data are included (Panel *H*), the full dataset best matches a Govardovskii opsin template with $lambda_{max}$ = 521 nm (MAE = 0.41; solid black line), assuming a correction for lens transmission of a 22-y-old individual; the best-fit opsin without lens transmission correction is shown in the dashed gray line for comparison ($lambda_{max}$ = 522 nm; MAE = 0.39).

some of the single- and dual-model interpretations differed. For example, including the 620 nm data strengthened the contribution of the L+M cones compared to the ipRGCs (Fig. 5 *C* and *F* and *SI Appendix*, Fig. S6 *C* and *F*). Importantly, however, in both of the three-channel models, the majority of the response was driven by the S cones (~50% contribution) with a peak at 445 nm (Fig. 5*G* and *SI Appendix*, Fig. S6*G*).

In contrast to the ED_{50} data, analysis of the ED_{90} value of the non-univariant fits (Fig. 4) suggested minimal contribution of the S cones for maximal phase resetting response, although the resulting action spectrum was poorly fit by our photoreceptor combination models (*SI Appendix*, Fig. S7).

Discussion

It is over twenty years since the discovery of melanopsin in the human eye (30) and the role of ipRGCs in orchestrating a wide range of responses to light (31). These 'non-visual' responses are fundamental to human physiology, mediating the daily resetting of the circadian pacemaker (32), regulating the amount of light entering the eye through pupil constriction (26, 33), providing alerting signals to the brain (34), and underpinning multiple therapeutic benefits of light to treat fatigue, depression, and circadian rhythm disorders among other conditions (e.g., refs. 35–38). While much work has been done to understand how the ipRGCs and visual photoreceptors interact, there remains ambiguity in how their contributions change with light intensity, pattern, timing, history, spectral distribution, and duration. The interaction with duration is of particular interest given that real-world light exposures are much longer than most experimentally studied light exposures, and thus, knowledge of the dynamics of light exposure with respect to duration is vital for translating basic experimental findings into usable benefits for health and safety. In the current study, we have extended our previous work examining the interplay between light irradiance, spectral distribution, and duration to identify the temporal and spectral dynamics of light responses. Our action spectra constructed from 6.5-h monochromatic light exposure data indicate that the relative contribution of cone photoreceptors to the melatonin suppression response is strongest at the beginning of a light exposure but declines over the first 1 to 3 h such that melanopsin from ipRGCs is the dominant contributor to detecting and transducing light information to the brain. This finding is consistent with a single-opsin best-fit $lambda_{max}$ of 481 nm and with a significant contribution of melanopsin (81%) to the best-fit linear combination of ipRGCs, S cones, and L+M cones for the circadian phase resetting response to a 6.5-h monochromatic light exposure.

The initial studies quantifying the spectral properties of melatonin suppression in response to 30- and 90-min exposures at night constructed analytic action spectra that did not fit the sensitivity curves for rod (scotopic)- or cone (photopic)-based phototransduction. These analyses assumed a univariant (i.e., single photoreceptor) response and predicted that an opsin with a peak sensitivity of ~460 nm mediated the short-duration melatonin suppression response (19, 20). Findings from our 2003 study, however, in which melatonin suppression was measured in response to exposure to a single photon density (2.8×10^{13} photons/cm^2/sec) of 460 nm or 555 nm monochromatic light over 6.5 h, were inconsistent with a single photoreceptor response because overall level of suppression and the time course of melatonin suppression recovery during the 555 nm light was greater than would be expected for a simple difference in spectral

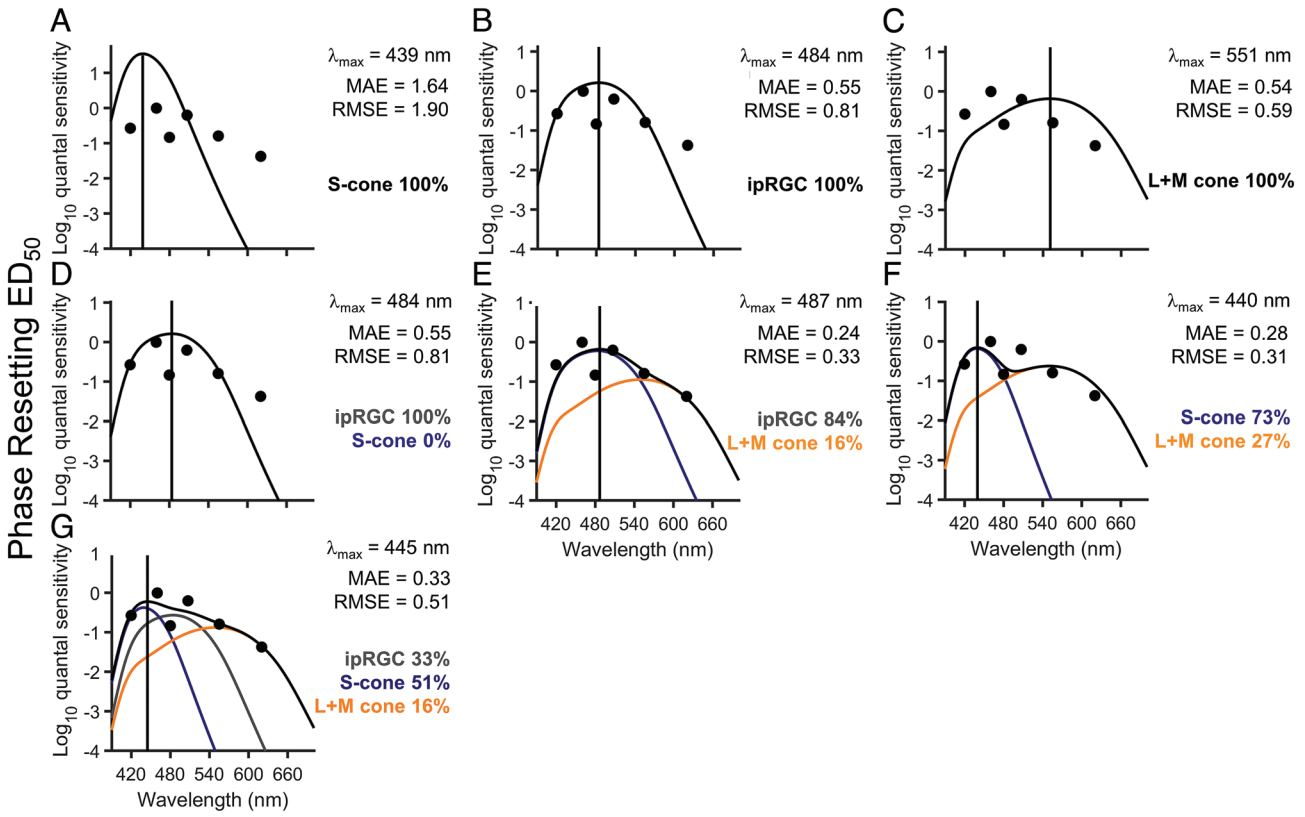

Fig. 5. Linear combinations of opsin fits to phase resetting across 6.5 h of light exposure. (*A–C*) The S-cone (*A*), ipRGC (*B*), and L+M opsin template (*C*) reflecting correction for lens transmission plotted against the relative quantum sensitivities derived from the $\log_{10}ED_{50}$ values for the overall 6.5-h light exposure for phase resetting with the data at 620 nm included in the fits. (*D–G*) The best-fit linear combinations of ipRGCs and S cones (*D*), ipRGCs and L+M cones (*E*), S cones and L+M cones (*F*), and ipRGCs, S cones, and L+M cones (*G*). In each panel, the gray solid line represents the ipRGC sensitivity curve, the blue solid line represents the S cone sensitivity curve, and the orange solid line represents the L+M cone sensitivity curve, whereas the black solid line shows the sum of the sensitivity curves, i.e., the best fit through the data points. The $lambda_{max}$ (vertical solid line) reported in each panel indicates the peak sensitivity of the best-fit sensitivity curve. The percentages represent the relative contribution of each spectral sensitivity curve to the overall sensitivity. The MAE and RMSE of the best fits are reported for each model.

sensitivity for a single photoreceptor (39). These experiments were later extended to include full irradiance response curves for 460 nm and 555 nm light and confirmed that multiple photoreceptor inputs were required to explain the differing time course of melatonin suppression, particularly the exponential decline (half-life ~38 min) in response to the 555 nm light, which represents the peak of the photopic sensitivity function (24). These data also showed that, at the start of a light exposure (first ~90 min), cone photoreceptors (represented by a single opsin with peak at 555 nm) appeared to contribute substantially to melatonin suppression, in contrast to the findings of the original human short-duration exposure action spectrum studies.

Although these comparisons of two specific wavelengths provided useful insight, the photobiological standard for identifying photoreceptor contributions is to generate an analytic action spectrum. In the current study, we generated such action spectra by constructing full fluence response curves for exposure to 6.5-h monochromatic light exposures at 420 nm, 480 nm, and 507 nm in addition to our published data at 460 nm and 555 nm. These wavelengths were chosen to be close to the peak sensitivity for the S cone, melanopsin, and rods, respectively. By constructing fluence response curves for a range of wavelengths, we could also examine different models of photoreceptor contributions rather than assuming a univariant response, as in the short-duration action spectra (19, 20). Our results suggest that cone photoreceptors contribute to melatonin suppression at the beginning of a light exposure (i.e., first 1 to 3 h). Thereafter, melanopsin dominates and can explain nearly the entire melatonin suppression response. The complex multi-photoreceptor contributions that we have reported (e.g., Fig. 3) may explain why published short-duration action spectra have a different peak than longer duration exposures (19, 20). The short-duration peak may represent a mixed response of cones and melanopsin contributions. Indeed, following a recent re-evaluation of these action spectra with additional data at shorter wavelengths (415 nm), it has been hypothesized that there is a strong S-cone contribution to short-duration (30 min) melatonin suppression (40), although the specific role of S-cones remains controversial (41). We also cannot rule out that our action spectrum models were overfit due to the small number of wavelengths available for analysis. We have tried to address this issue by including both the RMSE and MAE as model evaluation metrics (42), but further studies at additional wavelengths are needed to improve confidence in the model findings.

The inclusion of the 620 nm wavelength data in our analysis of the phase resetting response should be treated with caution due to the lack of a full fluence response curve (only n = 4), and the analyses excluding these data are reported in the *SI Appendix*, Fig. S6 given this concern. The relative role of red light on melatonin suppression and circadian resetting is not well defined. Prior studies have reported minimal effects of longer wavelength light on melatonin suppression but some evidence of a role for phase resetting responses. For example, Hanifin et al. (43) reported almost no melatonin suppression in response to 630 nm or 700 nm light. Similarly, both Zeitzer et al. (44) and Ho-Mien et al. (45) found

no melatonin suppression in response to red light but reported modest phase advances and phase delays, respectively. While inclusion or exclusion of the 620 nm data in our fits did not significantly change the overall estimates of the relative contribution of ipRGCs, S cones, and L+M cones when combined, further studies on the phase resetting effects of red light are warranted.

A recent review of the temporal dynamics of short- versus long-duration light exposures across several mammalian species (46) provides evidence for different temporal responses to light at short- and long-duration time scales. Our previous studies indicate that the phase resetting response is maximally sensitive to light over the first several minutes of light exposure (log/linear scale), and remains responsive to longer-duration light exposure at a reduced phase-resetting yield (linear/linear scale). The finding that melanopsin, S-cones, and L+M cones have roles in both the phase resetting response and the early part of melatonin suppression suggests that the initial log/linear response may possibly reflect cone function whereas the reduced but sustained linear/linear response may reflect melanopsin function. It should be noted, however, that we do not conclude from these findings that melatonin suppression and phase resetting are driven by different photoreceptor systems. The apparent enhanced S-cone response for phase resetting is a consequence of the fact that the first few minutes of the light exposure elicit a stronger phase resetting response than the end of the light exposure. We cannot perform the same serial quartile analysis for phase resetting as we have done for melatonin suppression to show that melanopsin dominates later in the phase resetting response because a phase shift can only be measured in humans in a discrete manner (i.e., by evaluating the timing of circadian phase on the day after light exposure). The studies needed to confirm that melanopsin dominates the phase resetting response in longer-duration light exposures are complex, and would need to control for S-cone and melanopsin activation at both shorter- and longer-duration light exposures. Until these studies are done, the parsimonious explanation is that melatonin suppression and phase resetting have similar temporal dynamics with respect to photoreceptor contribution. Further evidence of a dominant melanopsin response in humans for longer-duration exposures comes from our work in individuals with colorblindness (47) and totally visually blind individuals who retain 'non-visual' photoreception responses, including robust melatonin suppression, phase shifting, and pupil constriction responses to ocular light exposure (21–23, 26, 48, 49). In a repeat of our initial long-duration exposure (39), we exposed a totally visually blind man with intact circadian photoreception to equal photon densities of 460 nm and 555 nm light (22); while the 460 nm light induced a near-maximal melatonin suppression response for the entire 6.5-h exposure, the 555 nm light had no effect at all, confirming no functional cone photoreceptor input and demonstrating that melanopsin alone is sufficient to mediate a continuous long-duration response. Similar sensitivities were found for pupil constriction responses in the same patient (26): sustained pupil constriction was maintained in this patient but fast responses were not observed in response to intermittent light, nor at low irradiances, as compared to sighted controls, consistent with rodent rod/cone knockout models (25) and a human action spectrum for pupil constriction (22).

While the findings described above quantify the assumed contributions from cone- and melanopsin-based photoreception, a role for rods cannot be excluded (50–52). Examination of the fitted half-maximum value of each irradiance response curve shows that 507 nm light is more effective than 480 nm light at suppressing melatonin and resetting circadian phase (Figs. 1 and 4 and *SI Appendix*, Fig. S3). Our dataset does not have enough power, however, to differentiate the relative contribution of opsins with peaks at 480 nm and 507 nm, given their proximity, and we therefore chose to prioritize melanopsin given the preponderance of evidence on its role in mediating human circadian responses. Additional future experiments more specifically targeting responses to 480 nm and 507 nm light are required to quantify the potential role of rods.

One important difference between our study and prior studies that have constructed analytic action spectra is the background light to which participants are exposed in the hours and days leading up to the experimental light exposure. In both Brainard et al. (19) and Thapan et al. (20), for example, participants were admitted to the laboratory within a few hours of the start of the light exposure and had only a few hours of dim-light adaptation (< 10 lux). In contrast, in our study participants were exposed to <3 lux while awake and 0 lux during sleep for ~78 h prior to the experimental light exposure. We know from prior literature that three days of very dim light compared to typical indoor room illuminance amplifies both the melatonin suppression response (53–54) and the phase resetting response (55) to light. It is unknown, however, whether prior light history impacts the spectral sensitivity of the melatonin suppression or phase resetting responses.

A main limitation of our findings is that all participants were treated with a pupil dilator (0.5% cyclopentolate HCl) prior to each experimental light exposure to control for pupil constriction effects on the amount of light entering the eye. This is a standard photobiological technique that has been applied in other studies (e.g., refs. 19 and 20), but does not represent real-world light exposure conditions. In addition, we did not record whether maximum pupil dilation was maintained for the entire 6.5-h light exposure. It has been reported previously that a different formulation of this pupil dilator (1% cyclopentolate HCl) maintains maximal mydriatic response for at least 5 h (56). Prior findings from our group, however, indicate that the long-duration pupil constriction response in humans is driven by melanopsin (26). If the effects of the pupil dilator waned prior to the end of the 6.5-h light exposure, then any breakthrough pupil constriction that may have occurred in the latter part of the light exposure would have been stronger in response to wavelengths close to the melanopic peak of 480 nm. Given that the responses in the latter part of the light exposure indicate strong contributions from melanopsin despite this potential constriction, we do not think any possible waning effects of the pupil dilator are impacting our results in a way that would change our interpretation.

Given the ubiquity of light in our everyday lives, there is great interest in the application of experimental data to lighting practice, and we (57–60) and others (e.g., refs. 61–63) have made initial attempts to do so. Light duration has not yet been a key consideration in these efforts, but clearly, the spectral sensitivity of short-duration exposures is different from longer-duration exposures, and therefore translation of findings from short-duration exposures to longer photoperiods, or using melatonin suppression to predict other non-visual effects of light, may be premature, or at least less accurate (64, 65). While we acknowledge that a 6.5-h light exposure is not equivalent to the longer photoperiods experienced in real-world environments, such a light duration is more realistic than the shorter durations (e.g., 30- to 90-min exposures) previously studied. Our data therefore suggest that a conservative view be taken until unequivocal data prove otherwise, namely that when considering circadian resetting and melatonin suppression responses to light under typical exposure durations (i.e., during an overnight shift), melanopsin contributions are likely to predominate, and quantification of melanopsin stimulation should underpin lighting recommendations for real-world environments.

Materials and Methods

Participants. Healthy research subjects (n = 122), ages 18 to 30 y were enrolled in a 9-d inpatient study at the Intensive Physiologic Monitoring Unit (IPM) in the Center for Clinical Investigation (CCI) at Brigham and Women's Hospital (BWH; Boston, MA) between 2000 and 2009. There was approximately uniform distribution for date of admission to the inpatient study across spring (28%), summer (22%), autumn (28%), and winter (22%) across all wavelength groups. Physical health was assessed by medical history, physical examination, blood biochemistry and hematology, and electrocardiogram, and mental health was evaluated by interview with a staff psychologist/psychiatrist. Normal sight was confirmed by an ophthalmologic examination. Ishihara's test for color deficiency was administered to rule out red-green color deficiency and total color-blindness or weakness. Sleep and circadian rhythm disorders were exclusionary. For at least 2 wk prior to being admitted to the IPM, subjects were required to maintain a regular sleep-wake schedule (8 h sleep, 16 h wake), which was verified by continuous actigraphy monitoring (Actiwatch-L; Minimitter, Inc.). A comprehensive toxicology screen was performed on the day of admission to the IPM to ensure that subjects had refrained from the use of drugs. Of the 122 participants who were enrolled, 14 participants were discontinued prior to being randomized to the experimental light exposure. In addition, 11 participants were excluded from the melatonin suppression analysis and 10 participants were excluded from the phase resetting analysis due to insufficient samples. Results from 52 subjects (n = 24 460 nm, n = 24 555 nm, and n = 4 dark controls) were reported previously (24). In addition, two subjects from a similar study (66) who had comparable light exposure timing were included in the 480 nm group for the present analysis. Written informed consent was obtained from all participants. All research procedures were approved by the Institutional Review Board at BWH and were in compliance with HIPAA regulations and the Declaration of Helsinki.

Protocol Design. Participants lived in individual suites for 9 d in an environment free of time cues. A raster plot of the protocol is included in Fig. 1*A* of Gooley et al. (24). During the first 3 d, subjects were scheduled to sleep and wake at their regular pre-study sleep-wake times (8 h sleep, 16 h wake). Ambient light was provided by 4,100K fluorescent lamps (Philips Lighting). Participants lived in room light (<190 lux, 0.48 W/m^2 measured in the horizontal plane at 183 cm; melanopic EDI = 138 lux) until midway through day 3, after which the light was dimmed to <3 lux (<0.01 W/m^2; <2 melEDI lux) for the remainder of the study. After awakening on day 4, subjects underwent a 50-h constant routine procedure consisting of wakefulness enforced by technician monitors, semi-recumbent bed rest, and consumption of hourly equicaloric snacks. Following an 8-h sleep opportunity, subjects awoke in the evening and were administered a 6.5-h narrow-bandwidth light exposure (10 to 14 nm half-peak bandwidth) in a modified Ganzfeld dome. For the light exposure (day 6), a between-subjects design was used in which participants were assigned to one of six wavelength conditions (420 nm, 460 nm, 480 nm, 507 nm, 555 nm, or 620 nm) plus 4 dark controls. The data for 460 nm and 555 nm exposures have been reported previously (24). In each group, subjects were randomized to 4 to 16 irradiances across a broad range of photon densities (2.52×10^{11} to 1.53×10^{14} photons/cm^2/sec). Light was generated by a Xenon arc lamp and grating monochromator, and the wavelength and bandwidth were verified by measurement with a PR-650 SpectraColorimeter (PhotoResearch Inc.). Fifteen minutes prior to the onset of the light exposure, one drop of 0.5% cyclopentolate HCl was administered in each eye to dilate the pupils (Cyclogyl; Alcon Laboratories, Inc.). Head position was fixed by a chinrest, and subjects stared at the light continuously for 90 min at a time, followed by a 10-min break during which they could look elsewhere in the otherwise dark room. Participants were asked to refrain from photophobic behavior (e.g., squinting or closing of the eyes) and compliance was monitored by a technician. The light was measured every 30 to 60 min at eye-level with an IL1400 radiometer and SEL-033/F/W detector (International Light Inc.) to ensure constant irradiance throughout the light exposure. For each wavelength of light, participants were randomized to an irradiance level just prior to administration of the light exposure. Following completion of the light exposure and an 8-h sleep opportunity, subjects underwent a second constant routine for 30 h. After recovery sleep, subjects awoke on day 9 at their habitual wake time and were discharged from the study.

Specimen Collection and Melatonin Assays. On day 2 of the study, an indwelling intravenous catheter was inserted in a forearm vein to allow for continuous collection of blood during both sleep and wake episodes. During sleep episodes, the constant routine procedures, and the light exposure session, blood was drawn from outside the research suite through a porthole in the bedroom wall. Blood was sampled every 30 min during the constant routine procedures, and every 20 to 30 min during the 6.5-h light exposure. Saliva samples were collected hourly during the constant routines and the light intervention, and sample times were digitally time-stamped using a Termiflex system (Warner Power Termiflex). Melatonin concentration was determined by double-antibody radioimmunoassay with the Kennaway G280 antiserum by a laboratory blind to condition (Dr. V. Ricchiuti, BWH GCRC Core Laboratory, Boston, MA). The plasma melatonin intra-assay coefficient of variation (CV) was 10.0% at 1.9 pg ml^{-1} and 7.2% at 21.9 pg ml^{-1}, and the inter-assay CV was 12.65% at 3.06 pg ml^{-1} and 12.12% at 22.36 pg ml^{-1}. The saliva melatonin intra-assay CV was 4.1% at 3.56 pg ml^{-1} and 4.8% at 24.2 pg ml^{-1}, and the inter-assay CV was 12.15% at 2.37 pg ml^{-1} and 10.20% at 19.58 pg ml^{-1}.

Melatonin Suppression and Phase-Shift Responses. To determine percent suppression of melatonin, the area under the curve (AUC, trapezoidal method) was calculated for melatonin during the 6.5-h light exposure (AUC_{LE}) and compared to the AUC for the melatonin rhythm during the preceding constant routine at the same relative clock times (AUC_{CR1}). Thus, percent melatonin suppression was calculated as $[1 - (AUC_{LE})(AUC_{CR1})^{-1}] \times 100$, whereby higher values indicated stronger suppression of the melatonin rhythm. Melatonin suppression was calculated from plasma melatonin in 89 subjects (420 nm, n = 8; 460 nm, n = 29; 480 nm, n = 10; 507 nm, n = 7; 555 nm, n = 29; 620 nm, n = 2; dark controls, n = 4), and from salivary melatonin in 10 subjects (420 nm, n = 1; 460 nm, n = 1; 480 nm, n = 1; 507 nm, n = 1; 555 nm, n = 4; 620 nm, n = 2) because there was an insufficient number of blood samples collected during either the constant routine or light exposure from which to calculate suppression.

To determine the magnitude of phase-shift responses, the pre-light exposure melatonin rhythm during the first constant routine procedure was fit by a 3-harmonic regression model to estimate the amplitude. The dim light melatonin onset ($DLMOn_{25\%}$) was defined as the clock time at which the melatonin rhythm crossed a threshold value of 25% of the peak-to-trough fitted amplitude (half the standard amplitude). The phase-shift of the melatonin rhythm was calculated as the difference in the timing of the $DLMOn_{25\%}$, measured before and after the light exposure intervention using constant routine procedures (days 5 and 7). Phase-shifts were determined from plasma melatonin in 89 subjects (420 nm, n = 9; 460 nm, n = 29; 480 nm, n = 11; 507 nm, n = 7; 555 nm, n = 27; 620 nm, n = 2; dark controls, n = 4) and from salivary melatonin in 11 subjects (420 nm, n = 1; 460 nm, n = 2; 480 nm, n = 1; 507 nm, n = 1; 555 nm, n = 4; 620 nm, n = 2) because there was an insufficient number of blood samples collected during either the first or second constant routine. By convention, phase delays are indicated by negative values and phase advances by positive values.

Construction of Dose-Response Curves. Dose-response curves were fit with a sigmoidal four-parameter logistic regression model wherein A_1 is the minimum response, $A_2$is the maximum response, x_0 is the $\log_{10}$ irradiance that elicits a half-maximal response (i.e., the ED_{50} value), and p is the slope parameter:

$$y = A_2 + \frac{A_1 - A_2}{1 + \left(\frac{x}{x_0}\right)^p}$$

For non-univariant fits, A_1 and A_2 were fixed (at 0 and 95% for melatonin suppression and 0.05 and −3.3 for phase resetting, respectively) while x_0 and p were allowed to vary. To examine the dose-response of melatonin suppression across time, we constructed dose-response curves in quarterly (1 quarter = 97.5 min) bins across the 6.5-h light exposure. When a melatonin sample did not occur precisely at the onset or offset of a bin, the concentration of melatonin was interpolated linearly from the samples that bracketed the given time-point. All logistic fits were conducted using the nonlinear curve fit function in OriginPro 8.5, which minimizes the deviation between the experimental data and the theoretical fit using chi-square minimization and the Levenberg–Marquardt (L-M) algorithm to adjust the parameter values in the iterative procedure. The

R^2 value was generated to report the amount of variance explained by the logistic relationship between the irradiance and the melatonin suppression or phase resetting response.

Construction of Action Spectra. An unknown photopigment can be approximated with a common template using only one parameter, the maximum absorbance wavelength lambda$_{max}$ (27). A series of sensitivity curves with peaks from 420 to 720 nm were derived using the Govardovskii template (28). The half-maximum $\log_{10}$ ED$_{50}$ values obtained from fitting the 4-parameter intensity response curves were normalized to the maximum value to calculate the relative quantum sensitivity across the tested wavelengths (420, 460, 480, 507, 555, and 620 nm), and compared to the series of sensitivity curves to determine the best-fit photopigment based on the curve with the smallest MAE and RMSE. To determine the relative contributions of ipRGCs, S cones, and L+M cones, we fit linear combinations based on the absorbance spectra of each photoreceptor. The low-density absorbance spectra of the S-cones, ipRGCs, M-cones, and L-cones were derived using the Govardovskii template with maximum absorbance wavelengths of 419 nm, 480nm, 531 nm, and 558 nm, respectively (12, 27, 28). As the available data were relatively sparse and the sensitivity of L- and M-cones have significant overlap, their response was modeled as a weighted sum using a 2:1 ratio (29), resulting in a maximum absorbance of 548 nm.

As the light exposure was measured in the corneal plane, all spectral sensitivity curves were corrected for pre-receptoral filtering. It is assumed that pupil diameter did not change the spectral retinal irradiance in these studies because all pupils were dilated prior to light exposure. The axial optical densities of peripheral cones were set to 0.2 (67). The total lens transmittance was estimated by using the average age of the participants involved in the study (22-y-old observer) using the total lens transmittance according to van de Kraats and van Norren (68), which causes a small shift in maximum absorbance toward longer wavelengths and a more realistic fit than the absorbance spectra of the photopigments. The influence of the macula was not considered.

For the 2-channel model, the contribution of ipRGCs and S-cones was modeled by the following linear combination:

$$S(\lambda) = \beta_1 S_{ipRGC}(\lambda) + \beta_2 S_S(\lambda)$$

where S(λ) is the overall spectral sensitivity curve, $S_{ipRGC}(\lambda)$ is the spectral sensitivity curve of the ipRGCs, λ_1 is the weight of the ipRGCs, $S_S(\lambda)$ is the spectral sensitivity curve of the S cones, and λ_2 is the weight of the S-cones. Similar equations were used for the ipRGC/L+M cone and S-cone/L+M cone linear combinations.

For the 3-channel model, the contribution of ipRGCs, S-cones, and L+M cones was modeled by the following linear combination:

$$S(\lambda) = \beta_1 S_{ipRGC}(\lambda) + \beta_2 S_S(\lambda) + \beta_3 S_{L,M}(\lambda)$$

where $S_{L,M}(\lambda)$ is the spectral sensitivity curve of the L+M cones, and λ_3 is the weight of the L+M-cones. The best fit of each linear combination to the relative quantum sensitivities for overall melatonin suppression, quarterly melatonin suppression, and overall phase resetting was determined using non-negative least squares (lsqnonneg function in MATLAB). The fitting procedure was carried out to minimize the error on a logarithmic scale, e.g.,

$$log_{10}ED_{50} = log_{10}\left(\beta_1 S_{ipRGC}(\lambda) + \beta_2 S_S(\lambda)\right) + \gamma$$

where γ is a normalization constant. The MAE and RMSE are reported to determine best-fit models, where smaller MAE and RMSE values indicate better fits.

Data, Materials, and Software Availability. De-identified individual data for all outcomes are provided in the Harvard Dataverse repository (10.7910/DVN/J49FV3) (69).

ACKNOWLEDGMENTS. We thank research volunteers, recruiters, and research staff at the Division of Sleep and Circadian Disorders, Brigham and Women's Hospital (BWH); the technical, dietary, nursing, and medical staff at the Center for Clinical Investigation at BWH in partnership with the Harvard Catalyst, Jonathan Williams MD, for medical supervision; Ralph Todesco (BWH) for administrative support; Joseph M. Ronda, M.A.S. (BWH) for technical support; John Hanifin, Ph.D. and William Coyle (Thomas Jefferson University) and Ron Kovak and Jon Cooke (Photon Technology International, Inc.) for technical support for the generation of monochromatic light; Vincent Ricchiuti, Ph.D. and the Core Laboratory staff (BWH) for melatonin assays. This study was supported by National Institutes of Health grants T32-HL007901 (MSH, J.J.G.), R01-MH045130 (C.A.C.), R01-NS036590 (G.C.B.), and R01-AT002129 (S.W.L.); Ecole Polytechnique Fédérale de Lausanne (M.L.A., M.A.); Swiss National Science Foundation grant CR13I2_153018 (M.L.A.); and National Space Biomedical Research Institute grants NBPF02001 (M.R., S.W.L.), HPF00001 (G.C.B., S.W.L.), HPF01605 (G.C.B.), HPF01701 (G.C.B.), HFP01601 (C.A.C.), and HPF01301 (S.W.L.) through NASA NCC 9–58. The project described was conducted through the Harvard Clinical and Translational Science Center from the National Center for Research Resources, which was supported by National Institutes of Health grants M01-RR01066 and 1UL1-RR025758. The content is solely the responsibility of the authors and does not necessarily represent the official views of the National Center for Research Resources, the National Center for Advancing Translational Science or the National Institutes of Health.

Author affiliations: [a]Division of Sleep and Circadian Disorders, Departments of Medicine and Neurology, Brigham and Women's Hospital, Boston, MA 02115; [b]Division of Sleep Medicine, Harvard Medical School, Boston, MA 02115; [c]Laboratory of Integrated Performance in Design, École Polytechnique Fédérale de Lausanne, CH-1015 Lausanne, Switzerland; [d]Turner Institute for Brain and Mental Health and School of Psychological Sciences, Monash University, Clayton, VIC 3000, Australia; [e]Department of Neurology, Sidney Kimmel Medical College, Thomas Jefferson University, Philadelphia, PA 19107; and [f]Neuroscience and Behavioral Disorders Program, Duke-NUS Medical School, Singapore 169857, Singapore

1. R. Y. Moore, The suprachiasmatic nucleus and the circadian timing system. *Prog. Mol. Biol. Transl. Sci.* **119**, 1–28 (2013).
2. R. Teclemariam-Mesbah, G. J. Ter Horst, F. Postema, J. Wortel, R. M. Buijs, Anatomical demonstration of the suprachiasmatic nucleus-pineal pathway. *J. Comp. Neurol.* **406**, 171–182 (1999).
3. R. J. Wurtman, J. Axelrod, L. S. Phillips, Melatonin synthesis in the Pineal gland: Control by light. *Science* **142**, 1071–1073 (1963).
4. A. J. Lewy, T. A. Wehr, F. K. Goodwin, D. A. Newsome, S. P. Markey, Light suppresses melatonin secretion in humans. *Science* **210**, 1267–1269 (1980).
5. J. J. Gooley *et al.*, Exposure to room light before bedtime suppresses melatonin onset and shortens melatonin duration in humans. *J. Clin. Endocrinol. Metab.* **96**, E463–E472 (2011).
6. A. M. Chang, D. Aeschbach, J. F. Duffy, C. A. Czeisler, Evening use of light-emitting eReaders negatively affects sleep, circadian timing, and next-morning alertness. *Proc. Natl. Acad. Sci. U.S.A.* **112**, 1232–7 (2015).
7. Z. M. Weil, J. C. Borniger, Y. M. Cisse, B. A. Abi Salloum, R. J. Nelson, Neuroendocrine control of photoperiodic changes in immune function. *Front Neuroendocrinol.* **37**, 108–118 (2015).
8. B. Claustrat, J. Leston, Melatonin: Physiological effects in humans. *Neurochirurgie* **61**, 77–84 (2015).
9. A. D. Güler *et al.*, Melanopsin cells are the principal conduits for rod-cone input to non-image-forming vision. *Nature* **453**, 102–105 (2008).
10. S. Hattar *et al.*, Melanopsin and rod-cone photoreceptive systems account for all major accessory visual functions in mice. *Nature* **424**, 76–81 (2003).
11. S. Panda *et al.*, Melanopsin is required for non-image-forming photic responses in blind mice. *Science* **301**, 525–527 (2003).
12. D. M. Berson, F. A. Dunn, M. Takao, Phototransduction by retinal ganglion cells that set the circadian clock. *Science* **295**, 1070–1073 (2002).
13. J. J. Gooley, J. Lu, T. C. Chou, T. E. Scammell, C. B. Saper, Melanopsin in cells of origin of the retinohypothalamic tract. *Nat. Neurosci.* **4**, 1165 (2001).
14. K. Y. Wong, F. A. Dunn, D. M. Graham, D. M. Berson, Synaptic influences on rat ganglion-cell photoreceptors. *J. Physiol.* **582**, 279–296 (2007).
15. M. A. Belenky, C. A. Smeraski, I. Provencio, P. J. Sollars, G. E. Pickard, Melanopsin retinal ganglion cells receive bipolar and amacrine cell synapses. *J. Comp. Neurol.* **460**, 380–393 (2003).
16. D. M. Dacey *et al.*, Melanopsin-expressing ganglion cells in primate retina signal colour and irradiance and project to the LGN. *Nature* **433**, 749–754 (2005).
17. S. Panda *et al.*, Melanopsin (Opn4) requirement for normal light-induced circadian phase shifting. *Science* **298**, 2213–2216 (2002).
18. N. F. Ruby *et al.*, Role of melanopsin in circadian responses to light. *Science* **298**, 2211–2213 (2002).
19. G. C. Brainard *et al.*, Action spectrum for melatonin regulation in humans: evidence for a novel circadian photoreceptor. *J. Neurosci.* **21**, 6405–6412 (2001).
20. K. Thapan, J. Arendt, D. J. Skene, An action spectrum for melatonin suppression: evidence for a novel non-rod, non-cone photoreceptor system in humans. *J. Physiol.* **535**, 261–267 (2001).
21. C. A. Czeisler *et al.*, Suppression of melatonin secretion in some blind patients by exposure to bright light. *N. Engl. J. Med.* **332**, 6–11 (1995).
22. F. H. Zaidi *et al.*, Short-wavelength light sensitivity of circadian, pupillary, and visual awareness in humans lacking an outer retina. *Curr. Biol.* **17**, 2122–2128 (2007).
23. J. T. Hull, C. A. Czeisler, S. W. Lockley, Suppression of Melatonin secretion in totally visually blind people by ocular exposure to white light: Clinical characteristics. *Ophthalmology* **125**, 1160–1171 (2018).
24. J. J. Gooley *et al.*, Spectral responses of the human circadian system depend on the irradiance and duration of exposure to light. *Sci. Transl. Med.* **2**, 31ra33 (2010).

25. R. J. Lucas *et al.*, Diminished pupillary light reflex at high irradiances in melanopsin-knockout mice. *Science* **299**, 245–247 (2003).
26. J. J. Gooley *et al.*, Melanopsin and rod-cone photoreceptors play different roles in mediating pupillary light responses during exposure to continuous light in humans. *J. Neurosci.* **32**, 14242–14253 (2012).
27. H. J. Dartnall, The interpretation of spectral sensitivity curves. *Br. Med. Bull.* **9**, 24–30 (1953).
28. V. I. Govardovskii, N. Fyhrquist, T. Reuter, D. G. Kuzmin, K. Donner, In search of the visual pigment template. *Vis. Neurosci.* **17**, 509–528 (2000).
29. L. T. Sharpe, A. Stockman, W. Jagla, H. Jägle, A luminous efficiency function, V*(lambda), for daylight adaptation. *J. Vis.* **5**, 948–968 (2005).
30. I. Provencio *et al.*, A novel human opsin in the inner retina. *J. Neurosci.* **20**, 600–605 (2000).
31. A. S. Fisk *et al.*, Light and cognition: Roles for circadian rhythms, sleep, and arousal. *Front. Neurol.* **9**, 56 (2018).
32. C. A. Czeisler, J. J. Gooley, Sleep and circadian rhythms in humans. *Cold Spring Harb. Symp. Quant. Biol.* **72**, 579–597 (2007).
33. A. V. Rukmini, D. Milea, T. Aung, J. J. Gooley, Pupillary responses to short-wavelength light are preserved in aging. *Sci. Rep.* **7**, 43832 (2017).
34. C. Cajochen, Alerting effects of light. *Sleep Med. Rev.* **11**, 453–464 (2007).
35. G. Glickman, B. Byrne, C. Pineda, W. W. Hauck, G. C. Brainard, Light therapy for seasonal affective disorder with blue narrow-band light-emitting diodes (LEDs). *Biol. Psychiatry.* **59**, 502–507 (2006).
36. J. L. Anderson, C. A. Glod, J. Dai, Y. Cao, S. W. Lockley, Lux vs. wavelength in light treatment of seasonal affective disorder. *Acta Psychiatr. Scand.* **120**, 203–212 (2009).
37. K. L. Sinclair, J. L. Ponsford, J. Taffe, S. W. Lockley, S. M. Rajaratnam, Randomized controlled trial of light therapy for fatigue following traumatic brain injury. *Neurorehabil. Neural Repair.* **28**, 303–313 (2014).
38. J. J. Gooley, Treatment of circadian rhythm sleep disorders with light. *Ann. Acad. Med. Singap.* **37**, 669–676 (2008).
39. S. W. Lockley, G. C. Brainard, C. A. Czeisler, High sensitivity of the human circadian melatonin rhythm to resetting by short wavelength light. *J. Clin. Endocrinol. Metab.* **88**, 4502–4505 (2003).
40. T. M. Brown, K. Thapan, J. Arendt, V. L. Revell, D. J. Skene, S-cone contribution to the acute melatonin suppression response in humans. *J. Pineal Res.* **71**, e12719 (2021).
41. M. Spitschan, R. Lazar, E. Yetik, C. Cajochen, No evidence for an S cone contribution to acute neuroendocrine and alerting responses to light. *Curr. Biol.* **29**, R1297–R1298 (2019).
42. H. Pham, A new criterion for model selection. *Mathematics* **7**, 1215 (2019).
43. J. P. Hanifin *et al.*, High-intensity red light suppresses melatonin. *Chronobiol. Int.* **23**, 251–268 (2006).
44. J. M. Zeitzer, R. E. Kronauer, C. A. Czeisler, Photopic transduction implicated in human circadian entrainment. *Neurosci. Lett.* **232**, 135–138 (1997).
45. I. Ho Mien *et al.*, Effects of exposure to intermittent versus continuous red light on human circadian rhythms, melatonin suppression, and pupillary constriction. *PLoS One* **9**, e96532 (2014).
46. Cross-species consistencies and differences, R. E. Kronauer, M. A. St Hilaire, S. A. Rahman, C. A. Czeisler, E. B. Klerman, An exploration of the temporal dynamics of circadian resetting responses to short- and long-duration light exposures. *J. Biol. Rhythms.* **34**, 497–514 (2019).
47. F. L. Ruberg *et al.*, Melatonin regulation in humans with color vision deficiencies. *J. Clin. Endocrinol. Metab.* **81**, 2980–2985 (1996).
48. E. B. Klerman *et al.*, Nonphotic entrainment of the human circadian pacemaker. *Am. J. Physiol.* **274**, R991–R996 (1998).
49. G. Vandewalle *et al.*, Blue light stimulates cognitive brain activity in visually blind individuals. *J. Cogn. Neurosci.* **25**, 2072–2085 (2013).
50. G. S. Lall *et al.*, Distinct contributions of rod, cone, and melanopsin photoreceptors to encoding irradiance. *Neuron* **66**, 417–428 (2010).
51. R. J. Lucas, G. S. Lall, A. E. Allen, T. M. Brown, How rod, cone, and melanopsin photoreceptors come together to enlighten the mammalian circadian clock. *Prog. Brain Res.* **199**, 1–18 (2012).
52. A. Tikidji-Hamburyan *et al.*, Rods progressively escape saturation to drive visual responses in daylight conditions. *Nat. Commun.* **8**, 1813 (2017).
53. M. Hébert, S. K. Martin, C. Lee, C. I. Eastman, The effects of prior light history on the suppression of melatonin by light in humans. *J. Pineal Res.* **33**, 198–203 (2002).
54. K. A. Smith, M. W. Schoen, C. A. Czeisler, Adaptation of human pineal melatonin suppression by recent photic history. *J. Clin. Endocrinol. Metab.* **89**, 3610–3614 (2004). Erratum: *J. Clin. Endocrinol. Metab.* **90**, 1370 (2005).
55. A. M. Chang, F. A. Scheer, C. A. Czeisler, D. Aeschbach, Direct effects of light on alertness, vigilance, and the waking electroencephalogram in humans depend on prior light history. *Sleep* **36**, 1239–1246 (2013).
56. K. Lahdes *et al.*, Plasma concentrations and ocular effects of cyclopentolate after ocular application of three formulations. *Br. J. Clin. Pharmacol.* **35**, 479–483 (1993).
57. C. S. Pechacek, M. Andersen, S. W. Lockley, Preliminary method for prospective analysis of the circadian efficacy of (Day)light with applications to healthcare architecture. *LEUKOS* **5**, 1–26 (2018).
58. M. Andersen, J. Mardaljevic, S. W. Lockley, A framework for predicting the non-visual effects of daylight –Part I: Photobiology-based model. *Lighting Research and Technology* **44**, 37–53 (2012).
59. M. Andersen, A. Guillemin, M. L. Ámundadóttir, S. F. Rockcastle, "Beyond illumination: An interactive simulation framework for non-visual and perceptual aspects of daylighting performance BS2013" in *13th International Conference of the International Building Performance Simulation Association,* E. Wurtz, Ed. (International Building Performance Simulation Association (IBPSA), Chambéry, France, 2013), pp. 2749–2756.
60. M. L. Amundadottir, S. W. Lockley, M. Andersen, Unified framework to evaluate non-visual spectral effectiveness of light for human health. *Lighting Res. Technol.* **49**, 673–696 (2016).
61. E. C. Brawley, Enriching lighting design. *NeuroRehabilitation* **25**, 189–199 (2009).
62. M. G. Figueiro, R. D. White, Health consequences of shift work and implications for structural design. *J. Perinatol.* **33**, S17–S23 (2013).
63. C. Papatsimpa, J. P. Linnartz, Personalized office lighting for circadian health and improved sleep. *Sensors (Basel)* **20**, 4569 (2020).
64. S. A. Rahman *et al.*, Diurnal spectral sensitivity of the acute alerting effects of light. *Sleep* **37**, 271–281 (2014).
65. S. A. Rahman, M. A. St Hilaire, S. W. Lockley, The effects of spectral tuning of evening ambient light on melatonin suppression, alertness and sleep. *Physiol. Behav.* **177**, 221–229 (2017).
66. M. Rüger *et al.*, Human phase response curve to a single 6.5 h pulse of short-wavelength light. *J. Physiol.* **591**, 353–363 (2013).
67. L. T. Sharpe, A. Stockman, H. Jägle, H. Knau, J. L. Nathans, M and L-M hybrid cone photopigments in man: deriving lambda max from flicker photometric spectral sensitivities. *Vision Res.* **39**, 3513–3525 (1999).
68. D. van Norren, J. van de Kraats, Spectral transmission of intraocular lenses expressed as a virtual age. *Br. J. Ophthalmol.* **91**, 1374–1375 (2007).
69. M. A. St Hilaire, M.L. Ámundadóttir, S. A. Rahman, S. M. W. Rajaratnam, M. Rüger, G. C. Brainard, C. A. Czeisler, M. Andersen, J. J. Gooley, S. W. Lockley, The spectralsensitivity of human circadian phase resetting and melatonin suppression tolight changes dynamically with light duration. *Harvard Dataverse.* 10.7910/DVN/J49FV3. Deposited 26 August 2022.